Kalman filtered GPS accelerometerbased accident detection and location system: A low-cost approach

Article *in* Current science · June 2014

CITATIONS
10

READS
1,571

4 authors, including:

Md. Syedul Amin

31 PUBLICATIONS **167** CITATIONS

SEE PROFILE

Mamun Bin Ibne Reaz

Universiti Kebangssan Malaysia

305 PUBLICATIONS **2,978** CITATIONS

SEE PROFILE

Mohammad Arif Sobhan Bhuiyan

Xiamen University Malaysia

62 PUBLICATIONS **283** CITATIONS

SEE PROFILE

Kalman filtered GPS accelerometer-based accident detection and location system: a low-cost approach

Md. Syedul Amin, Mamun Bin Ibne Reaz, Mohammad Arif Sobhan Bhuiyan and Salwa Sheikh Nasir

Department of Electrical, Electronic and Systems Engineering, Universiti Kebangsaan Malaysia, 43600 UKM, Bangi, Selangor, Malaysia

A low-cost accident detection system utilizing cheap ADXL345 accelerometers and GPS receiver is proposed in this communication. The accident detection algorithm was developed based on sudden deceleration. The double integration of the acceleration and heading from the tilt angles of accelerometers were used to determine the location. Kalman filter was utilized to correct the accumulated double integration errors with the trusted GPS data. The field tests demonstrated the correct functioning of the accident detection algorithm and location. The proposed low-cost system can save many lives by the automated accident detection and accurate location even during GPS outage.

Keywords: Accelerometer, accident detection, GPS recovers, Kalman filter.

THE automobile is one of the greatest inventions that has become an essential part of our daily activities. However, it can bring about disaster and can even kill us through accidents. Vehicle accident is a vital problem in today's world[1]. Nearly 1.3 million people die in road crashes each year, which is 3,287 deaths per day and leaving 20–50 million injured or disabled[2]. Despite various efforts by different agencies against careless driving, accidents are taking place. About 6% of the accident fatalities could have been eliminated if the accident information had been divulged at the right time[3]. This can be achieved by an efficient automatic accident detection and notification system with correct location of the accident.

Accident detection system is a widely researched topic. Real-time traffic accident prediction relates accident occurrences from various detectors such as induction loops, infrared detector, camera, etc. However, these are restricted by the number of sensors, algorithms, traffic flow, weather, etc. Driver-initiated incident detection system has more advantages than manual incident detection system. However, during an accident, the driver may not be in a physical condition to report the accident manually. Chuan-Zhi *et al.*[4] proposed a freeway incident detection system utilizing the car air bag sensor and accelerometer, GPS to locate the place of accident and GSM to send the accident location. However, car air bag sensors are not installed in all cars and the location, at times, may not be known due to GPS outage.

A smart phone-based accident detection system has been proposed by White *et al.*[5] based on expensive smart phones and suffers from the possibility of false alarm. An impact sensor-based accident detection and wireless module-based reporting system proposed by Megalingam *et al.*[6] largely depends on the huge installation of wireless receiver at short intervals. A solely GPS-based accident detection and location system was proposed by Amin *et al.*[7]. The speed capability of GPS was used for accident detection and accident location was reported from GPS position through GSM. However, the proposed system suffers from the conventional limitations of the GPS. Sando *et al.*[8] also reported the limitations of GPS for locating a crashed vehicle.

The GPS receiver determines position by the direct line-of-sight signal from the satellites. The blockage by any obstruction affects both the amplitude and phase of the received satellite signals and needs requisition of satellite signals[9–11]. Moreover, the update rate of GPS is also not sufficient to determine the acceleration from the speed data for the purpose of accident detection. An accelerometer, on the other hand, provides instantaneous acceleration with higher update rate. Besides, it can also provide orientation information[12]. The rapid development of semiconductor manufacturing technologies enabled the development of MEMS-based accelerometers. However, the accuracy of the MEMS-based accelerometers is affected by accumulated bias, scale factor, drift, noise, etc. which vary with the price[13]. The limitation of instantaneous acceleration and outage of GPS can be overcome by the higher update rate of acceleration and orientation of the accelerometer. On the other hand, the inherited inaccuracy of the low-cost accelerometer can be overcome by accurate information of the GPS.

This communication proposes a low-cost, efficient, accident detection and location system utilizing cheap MEMS 3-axes accelerometers and GPS. The loosely coupled integration of accelerometer and GPS with Kalman filter provides proper acceleration information to detect accidents accurately and orientation of the vehicle for its exact location during GPS outage.

The GPS receiver determines the position by calculating the geometric intersection of the ranges of known coordinates of the satellites and the receiver using eq. (1) below[14]. At least four pseudorange measurements are required to estimate the position as eq. (1) has four unknowns (x, y, z and b). In low-cost GPS receivers, inexpensive quartz crystal oscillator is used as a timer. As such, the receiver clock drifts from true GPS time. So, eq. (1) includes a significant user time bias.

$$\rho_c^{(k)} = \sqrt{(x^{(k)} - x)^2 + (y^{(k)} - y)^2 + (z^{(k)} - z)^2} + b + \tilde{\varepsilon}_\rho^{(k)}, \quad (1)$$

*For correspondence. (e-mail: syedul8585@yahoo.com)

where $x^{(k)}$, $y^{(k)}$ and $z^{(k)}$ are the coordinates of the satellite, x, y and z are the user coordinates, b is the bias of the user clock and ε is the error source.

The receiver estimates velocity utilizing the Doppler shift between the satellites and the receiver. The Doppler shift can be determined with the known satellite velocity by differentiating pseudorange measurement. The pseudorange rate can be calculated using eq. (2). With minimum four pseudorange rate measurements, the velocity is determined using the least squares estimation. The acceleration (a) can be easily calculated from eq. (3), where dv is the change of velocity in time dt. However, the update rate of the low-cost GPS receivers is normally limited. As such, the instantaneous acceleration cannot be found from the GPS. Moreover, the acceleration is contaminated if the velocity is less than 1.5 m/s (ref. 12).

$$\rho^{(k)} = (v^{(k)} - v) \cdot 1^{(k)} + b + \varepsilon_{\varphi}^{(k)}, \tag{2}$$

$$a = \frac{\mathrm{d}v}{\mathrm{d}t}, \tag{3}$$

where $v^{(k)}$ is the satellite velocity vector, v is user velocity vector, b is rate of change of receiver clock, $1^{(k)}$ is the line-of-sight unit vector of the user-to-satellite unit and ε is the error source.

Digital accelerometer provides acceleration information in inter-integrated circuit (I^2C) or serial peripheral interface (SPI) protocol. The accelerometer reading needs to be scaled to the G values. The scale is calculated by dividing the total range with the number of bits as shown in eq. (4), where a_r is the total range and a_b is the number of bits. The acceleration in G can then be determined by multiplying the raw digital values by the scale. From the acceleration, the position can be found by eq. (5), where the present position is the summation of the previous position, integral of velocity and the double integration of the acceleration. During a constant velocity, the acceleration will be zero. Thus, the third term in eq. (5) will become zero. In this situation, the vehicle will move with a constant velocity and the position will be the summation of previous position and the integral of constant velocity as given in eq. (6).

$$\text{Scale} = \frac{a_r}{a_b}, \tag{4}$$

$$\vec{x}_t = \vec{x}_{t-1} + \int_{t-1}^{t} \dot{\vec{x}}\, \mathrm{d}t + \int_{t-1}^{t} \left(\int_{t-1}^{t} \ddot{\vec{x}}\, \mathrm{d}t \right) \mathrm{d}t, \tag{5}$$

$$\vec{x}_t = \vec{x}_{t-1} + \int_{t-1}^{t} \dot{\vec{x}}\, \mathrm{d}t. \tag{6}$$

The accelerometer provides acceleration due to movement and also acceleration due to gravity. By measuring the static acceleration caused by gravity, the tilt angle can be calculated. The tilt angle can provide the heading information of the vehicle. With three-axes accelerometers, the tilt angle can be determined using eq. (7) for an axis where X, Y and Z are the accelerations in x, y and z axes.

$$Ax = \arctan\left(\frac{X}{\sqrt{Y^2 + Z^2}} \right). \tag{7}$$

The accelerometer measurements need to be alignned with GPS measurements for the GPS and accelerometer fusion. Thus, the acceleration readings need to be transformed to the earth frame by a fixed rotation matrix. The vehicle position is expressed in x, y and z axis. It is expressed in geodetic coordinate frame. GPS uses a set of fundamental parameters referred by the World Geodetic System 1984 (WGS 84), where the ECEF (earth centred earth fixed) coordinate frame is for the GPS[14]. The transformation from LLA (ϕ, λ, h) to ECEF (x, y, z) is given in eq. (8), where N is called the normal, h the distance from the surface to the z-axis along the ellipsoid normal and e is the first numerical eccentricity of the ellipsoid.

$$\begin{bmatrix} x \\ y \\ z \end{bmatrix} = \begin{bmatrix} (N+h)\cos\phi\cos\lambda \\ (N+h)\cos\phi\sin\lambda \\ (N(1-e^2)+h)\sin\phi \end{bmatrix}. \tag{8}$$

The NED (north east down) is a right-handed coordinate system fixed to the vehicle which points to the true north, east and downward directions. The body coordinate frame is located at the centre of gravity (CG) of the vehicle, with x pointing towards the nose of the vehicle, y pointing towards the right door of the vehicle and z pointing down to comply with the right-hand rule. The different coordinate frames are shown in Figure 1. Equation (9) shows the primary rotation that brings the ECEF frame to coincide with NED frame and the vice versa is given in eq. (10). The NED to body frame coordinate rotation is given in eq. (11).

$$C_e^n = \begin{pmatrix} -\sin\phi\cos\lambda & -\sin\phi\sin\lambda & \cos\phi \\ -\sin\lambda & \cos\lambda & 0 \\ -\cos\phi\cos\lambda & -\cos\phi\sin\lambda & -\sin\phi \end{pmatrix}, \tag{9}$$

$$C_n^e = \begin{pmatrix} -\sin\phi\cos\lambda & -\sin\lambda & -\cos\phi\cos\lambda \\ -\sin\phi\sin\lambda & \cos\lambda & -\cos\phi\sin\lambda \\ \cos\phi & 0 & -\sin\phi \end{pmatrix}, \tag{10}$$

where ϕ is latitude and λ is longitude in geodetic frame.

$$C_b^n = \begin{pmatrix} c\theta c\psi & -c\phi s\psi + s\phi s\theta c\psi & s\phi s\psi + c\phi s\theta c\psi \\ c\theta s\psi & c\phi c\psi + s\phi s\theta s\psi & -s\phi c\psi + c\phi s\theta s\psi \\ -s\theta & s\phi c\theta & c\phi c\theta \end{pmatrix}, \quad (11)$$

where sin is denoted by s and cos is denoted by c.

Despite the accuracy of the GPS, it cannot provide location information during an outage. On the other hand, accelerometer can provide continuous acceleration which can be used to calculate the position. However, initialization with a valid GPS position is essential for the accelerometer to correctly determine accelerometer-derived position. But position and orientation of the accelerometer are contaminated by the double integration errors of the low-cost accelerometer. These limitations can be overcome by fusing both the sensor data with an appropriate filter. Kalman filter, particle filter, neural network, etc. are the popular filters for data fusion. However, Kalman filter is chosen in the proposed system due to its simplicity, computational efficiency and easier implementation compared to the other filters[15]. In spite of the predicted fused position from the Kalman filter, to restrict the error growth of the accelerometer-derived position, a valid GPS signal is needed from time to time.

Kalman filter is a recursive solution to discrete linear filtering which provides an optimal, unbiased method for estimation. Here, the state of a system[14] at time-step k is described by eq. (12) and updated with a measurement by eq. (13)

$$x_k = Ax_{k-1} + Bu_{k-1} + w_{k-1}, \quad (12)$$

$$z_k = Hx_k + v_k, \quad (13)$$

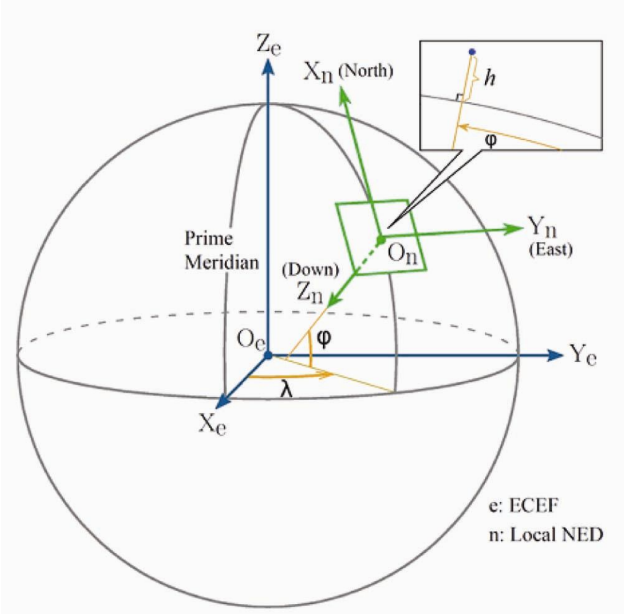

Figure 1. Geodetic, earth centred earth fixed (ECEF) and north east down (NED) coordinate system.

where the matrix A relates the state at time $k-1$ to the state at time k, matrix B relates the control input to the state, matrix H relates the state to the measurement, and variables v_k and w_k are the measurement noise and the process noise respectively.

The Kalman filter consists of five essential stages that repeat over a given time-interval. The current state estimate is used to compute the predicted value of the state at the next time interval by eq. (14). In the next stage, current state covariance estimate is used to compute the predicted value of the state covariance using eq. (15) at the next time-interval. The filter gain is computed using eq. (16). With the state estimate update, the posteriori state update is executed using eq. (17). In the final stage, the state covariance estimate is updated using eq. (18). The covariance and filter gain computation update can be done offline and the real-time Kalman filter implementation is reduced to state estimation only.

$$\hat{x}_k^- = A\hat{x}_{k-1} + Bu_{k-1}, \quad (14)$$

$$P_k^- = E\left[e_k^- e_k^{-T} \right], \quad (15)$$

$$K_k = P_k^- H^T (HP_k^- H^T + R)^{-1}, \quad (16)$$

$$\hat{x}_k^- = \hat{x}_k^- + K(Z_k - H\hat{x}_k^-), \quad (17)$$

$$P_k = E\left[e_k e_k^{-T} \right], \quad (18)$$

where $\hat{x}_k^-$ is the priori state estimate at step k, A an $n \times n$ matrix relating state at $k-1$ time to k, $\hat{x}_{k-1}$ the posteriori state estimate at time-step $k-1$, B the $n \times 1$ matrix relating the control input to state x, u a control input which is optional, P_k^- the priori estimate error covariance, and P_{k-1} the posteriori estimate error covariance.

The HI-204III GPS receiver (Haicom Electronics Corporation) is a low-cost device which provides satellite positioning data with a continuous tracking of all satellites in view. Its 4000 search bins and 20 parallel channels provide quick satellite signal acquisition and it takes less than 40 sec in cold start and 8 sec in hot start. With –159 dBm tracking sensitivity, it offers good navigation performance in urban areas and limited sky view with 1 Hz update rate.

The low-cost ADXL345 is an MEMS-based, small, thin, low power, three-axes accelerometer with high resolution (13-bit), which can provide measurement up to ±16 G. Its high resolution (4 mg/LSB) enables measurement of inclination changes less than 1.0°. An ATmega328 microprocessor is used at 57,600 bps to capture the ADXL345 data at ±8 g range in I^2C digital interface.

Raw accelerometer data were scaled to determine the acceleration data in G value using eq. (5). The scale was found to be 0.015625 with an acceleration range of ±8 G. The data were captured at 10bits. The raw value was multiplied by the G value (9.80665 m/s^2) after the scaling. The three-axes orthogonal accelerometers measure the longitudinal, latitudinal and gravitational acceleration respectively. The accelerometer data are rotated from the body frame to the NED frame using eq. (10). Data derived from the GPS lack in instantaneous acceleration, which is important in determining a sudden deceleration due to accident. But the accelerometer can provide instantaneous acceleration with high update rate which is the prime need for accident detection. As such, for the purpose of sudden deceleration detection the accelerometer data are only considered. But, the low-cost accelerometer data contain a lot of noise. Denoising is done using the Alaln variance method, low-pass filter and window of discrimination.

An efficient accident detection model is vital in detecting vehicle accident. A threshold-based filtering of deceleration is used to predict the occurrence of an accident. The accident detection scenario is activated when the vehicle travels above 23 kph. Speed below this is not likely to cause any fatal accident situation in frontal crash and reduces the false alarm of accident situation[16].

A vehicle decelerates when the brake is applied. The proposed system monitors the deceleration data from the accelerometer continuously. For the frontal crash, any deceleration more than 5 Gs is considered as an accident situation[17]. Once the deceleration is detected less than 5 Gs, the system checks for the velocity. In a frontal crash, the vehicle is likely to be stopped completely. If the velocity is found below 5 kph, then the system confirms it to be an accident. Considering the GPS and accelerometer conventional errors, the 5 kph velocity is considered. The velocity check after the deceleration threshold would reduce the chances of false alarm. Once the accident situation is detected, the system would raise an alarm for the location detection module. The flowchart of the accident detection is shown in Figure 2.

Beside the detection of the accident, the accelerometer can provide velocity information by integrating the acceleration once and the position information by double integration. The heading change can be found from the tilt angles of the accelerometers. However, the low-cost ADXL345 accelerometer suffers from noises and errors which include bias, random walk, quantization noise and jitter. This causes an error in the position which grows quadratically with time. The raw accelerometer data were collected for 24 h to determine the quantization noise, random walk, and bias instability of the accelerometer by fitting a curve to the resulting plot by the Allan variance method[18]. A window of discrimination between valid and invalid readings was used to remove the jitter around the stationary value using the errors from the Allan variance method. If the reading falls within these limits, then it is considered as noise and the acceleration is set to zero. The accelerometer also gives noisy data which come as a spike of sudden unusual acceleration for one or two samples. These are removed with a low-pass filter.

The loosely coupled GPS and accelerometer integration system with Kalman filter depends on the form of input data to the filter, which can be either three-dimensional velocity/position differences or pseudorange/rate differences. The three-dimensional velocity/position difference method is easier to implement due to its simple structure[19]. Thus, the difference of GPS-derived and accelerometer-generated velocity/position is taken as an input to the Kalman filter. The proposed Kalman filter integration of the GPS and accelerometer with its input and output is shown in Figure 3.

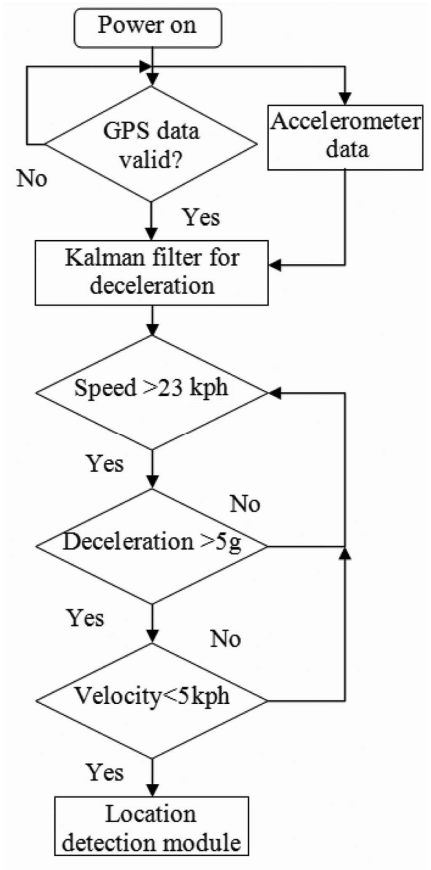

Figure 2. Accident detection algorithm.

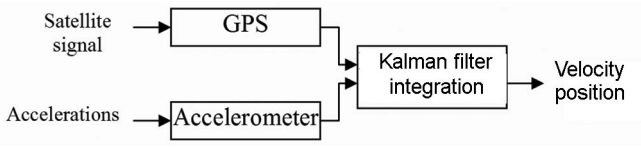

Figure 3. Proposed GPS and accelerometer integration by Kalman filter.

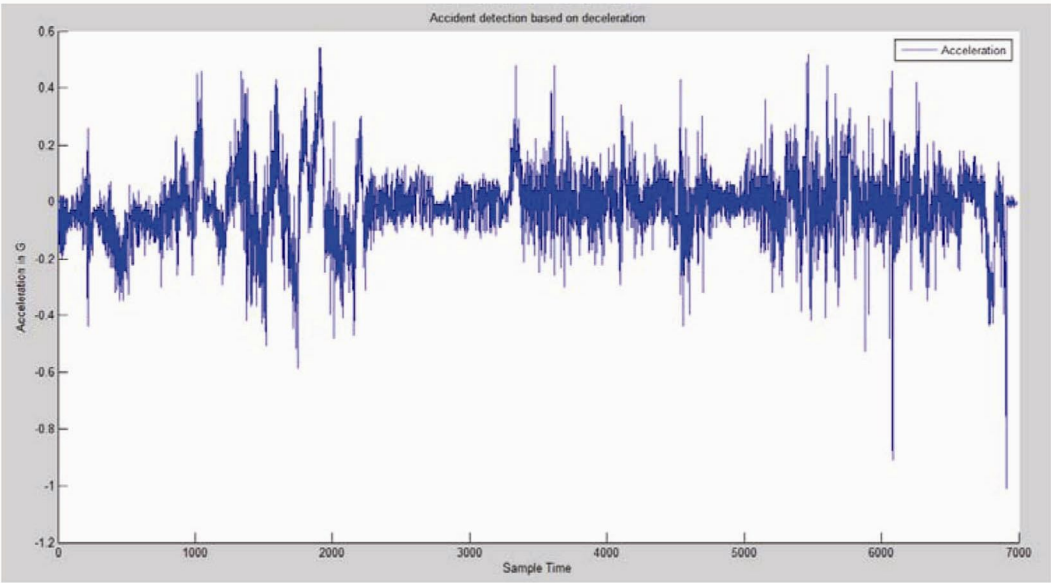

Figure 4. Accident detection based on deceleration.

The measurement error is an important parameter for the Kalman filter. As such, the measurement errors of the GPS and accelerometer need to be determined. The GPS velocity error is required to find the velocity measurement variance for observation equation. The standard deviation of the velocity measurement (σ_v) error can be found using eq. (19). The static velocity error (σ_{static}) was found to be 0.6 m/s by keeping the Haicom 204III GPS receiver static in a place with good line-of-sight for 3 h. The aggressive accelerations and decelerations for a vehicle[20] were considered to be 6 m/s^2. With the update rate of 1 m/s of the receiver, the dynamic velocity error (σ_{dynamic}) was found to be 6 m/s. A higher update rate GPS can reduce this error with an increment in the receiver price. Using eq. (19), the standard deviation (σ_v) of the velocity error is found to be 6.6 m/s

$$\sigma_v = \sigma_{\text{static}} + \sigma_{\text{dynamic}}. \tag{19}$$

The acceleration from the longitudinal axis accelerometer was integrated once to obtain the longitudinal velocity and integrated again to determine the displacement using eq. (5). The lateral accelerometer was used to determine the heading change using eq. (6). With the heading information, the east and north distances were calculated and the vehicle positions were determined using eqs (20) and (21).

$$\text{lat} = \text{lat} + (n\_\text{dist} * \text{degrees/m}), \tag{20}$$

$$\text{long} = \text{long} + (e\_\text{dist} * \text{degrees/m}). \tag{21}$$

After determining the measurement errors and position information for the GPS and the accelerometer, the data were fed to a Kalman filter using Matlab. The GPS data were reliable as the data do not contain long-term accuracy errors. The accelerometer errors were corrected using the GPS data. Whenever the GPS velocity information was more than 1.5 m/s, the position vector was updated by eq. (22). If the GPS velocity was not reliable (velocity < 1.5 m/s), then the position information was updated with the Kalman filter-derived accelerometer information using eq. (23), where A denotes accelerometer and G denotes for GPS.

$$\vec{X}(t) = \vec{X}(t-1) + \vec{V}_G \Delta t, \tag{22}$$

$$\vec{x}_t = \vec{x}_{t-1} + (\dot{\vec{x}}^G_{t-1} * \Delta t) + \left(\frac{1}{2}\ddot{\vec{x}}^A_t * (\Delta t)^2\right) + \left(\left(\frac{1}{2}\ddot{\vec{x}}^G_{t-1} * (\Delta t)^2\right) - \left(\frac{1}{2}\ddot{\vec{x}}^A_{t-1} * (\Delta t)^2\right)\right). \tag{23}$$

A test vehicle was used to evaluate the proposed system. The GPS was installed on the dashboard of the test vehicle for a better line-of-sight. The ADXL345 accelerometer was rigidly fixed at the middle of the vehicle. GPS and accelerometer data were recorded while driving on the road of Jalan Temuan, Universiti Kebangsaan Malaysia, Bangi, Selangor, Malaysia. The vehicle was driven at various speeds to obtain high accelerations. The vehicle was abruptly brought to a dead stop by applying the brake to attain sudden decelerations. During driving, the GPS was intentionally covered few times to deprive the line-of-sight. It was even intentionally covered before the last deceleration to test the correctness of the location information derived from the accelerometer. After the vehicle came to a dead stop, the GPS was uncovered to allow it to

reacquire the satellite so that the validity of the accelerometer position could be evaluated.

The collected data were post-processed using MATLAB software. The ADXL345 acceleration data recorded for the *X*-axis (direction of the vehicle movement) were plotted to detect the acceleration and deceleration, as shown in Figure 4. In the proposed accident detection algorithm, the deceleration above 5 Gs is considered as an accident situation. But achieving 5 Gs is impossible without a real accident. As such, the threshold was reduced to 0.9 G to test the accident detection. Figure 4 shows that the vehicle achieved 0.9 G deceleration at around 6000th sample time, but again it started accelerating. As such, although the 0.9 G threshold was reached, the accident was not declared as the vehicle started moving more than 5 kph after achieving the deceleration. But at around 7000th sample time, the vehicle again achieved a deceleration more than 0.9 G. But this time, the vehicle was completely stopped and thus it was treated as an accident. As such, the system could detect sudden deceleration and differentiate a false accident situation.

After an accident is detected, the system determines the location of the vehicle. The GPS coverage was intentionally interrupted several times during the test drive as mentioned above. Specially, before the vehicle came to a dead stop with high deceleration, the GPS acquisition had been intentionally blocked for a longer time. The Kalman filtered accelerometers positions compensated these gaps. Figure 5 shows the GPS outage positions with the filled-up Kalman filtered accelerometer positions. The GPS was allowed to reacquire the satellite position after the vehicle came to a dead stop in the simulated accident situation. The GPS-based position and the Kalman filter-based accelerometer position almost coincided, as seen in Figure 5. The GPS positions and the Kalman filtered accelerometer positions were plotted in the open-source Quantum Geographic Information System (QGIS; Figure 6). The plotting on the QGIS also showed the correct positions of the vehicle during GPS outage, which indicated the correct functioning of the proposed system.

Thus, a low-cost accident detection and location system has been developed in this study utilizing only off-the-shelf, low-cost accelerometers and GPS receiver. The instantaneous and higher rate of the accelerometer was used to detect an accident due to sudden deceleration. The accident location module was developed by double integrating the erroneous data of the accelerometer with the inherited intermittent data of GPS using the Kalman filter. The field test showed the correct accident detection and the location during a GPS outage. The low-cost system will be suitable for all vehicles and will also save many lives by the automated detection of accident and location.

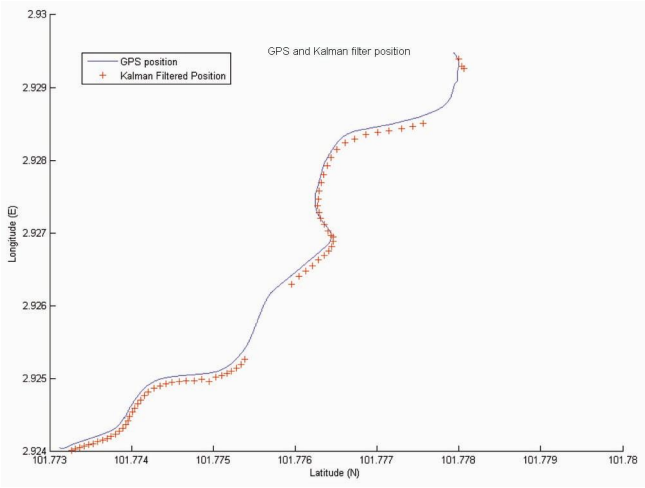

Figure 5. Kalman filtered accelerometer positions with GPS outage.

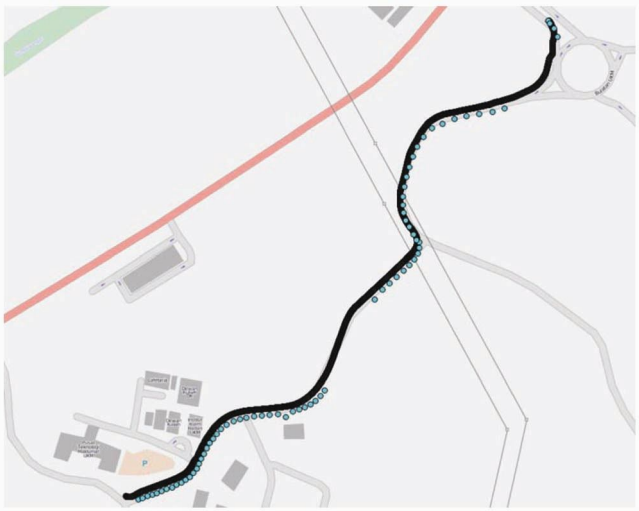

Figure 6. GPS and Kalman filtered accelerometer positions on Quantum Geographic Information System.

1. Surgailis, T., Valinevicius, A., Markevicius, V., Navikas, D. and Andriukaitis, D., Avoiding forward car collision using stereo vision system. *Electron. Electr. Eng.*, 2012, **18**(8), 37–40.
2. Annual Global Road Crash Statistics, 2013; http://www.asirt.org/KnowBeforeYouGo/RoadSafetyFacts/RoadCrashStatistics/tabid/213/Default.aspx (accessed on 20 March 2013).
3. Rauscher, S. *et al.*, Enhanced automatic collision notification system–improved rescue care due to injury prediction–first field experience. In Proceedings of the 21st International Technical Conference on the Enhanced Safety of Vehicles, Stuttgart, Germany, 2009.
4. Chuan-zhi, L., Ru-fu, H. and Hong-wu, Y. E., Method of freeway incident detection using wireless positioning. In IEEE International Conference on Automation and Logistics, Qingdao, China, 2008.
5. White, J., Thompson, C., Turner, H., Dougherty, B. and Schmidt, D. C., WreckWatch: automatic traffic accident detection and notification with smartphones. *Mobile Networks Appl.*, 2011, **16**(3), 285–303.
6. Megalingam, R. K., Nair, R. N. and Prakhya, S. M., Wireless vehicular accident detection and reporting system. In 2nd International Conference on Mechanical and Electrical Technology, Singapore, 2010.

7. Amin, M. S., Jalil, J. and Reaz, M. B. I., Accident detection and reporting system using GPS, GPRS and GSM technology. In International Conference on Informatics, Electronics & Vision, Dhaka, Bangladesh, 2012.
8. Sando, T., Mussa, R., Sobanjo, J. and Spainhour, L., GPS Usability in crash location. In ITE 2004 Annual Meeting and Exhibit, Lake Buena Vista, Florida, USA, 2004.
9. Sharma, S., Dashora, N., Galav, P. and Pandey, R., Cycle slip detection, correction and phase leveling of RINEX formatted GPS observables. *Curr. Sci.*, 2011, **100**(2), 205–212.
10. Song, X., Raghavan, V. and Yoshida, D., Matching of vehicle GPS traces with urban road networks. *Curr. Sci.*, 2010, **98**(12), 1592–1598.
11. Rao, G. S., Error analysis of satellite-based global navigation system over the low-latitude region. *Curr. Sci.*, 2007, **93**(7), 927–931.
12. Croyle, S. R., Spencer, L. E. and Sittaro, E. R., Vehicle navigation system and method using multiple axes accelerometer, Google Patents, 2001.
13. Goel, M., Electret sensors, filters and MEMS devices: New challenges in materials research. *Curr. Sci.*, 2003, **85**(4), 443–453.
14. Chaves, S. M., Using Kalman filtering to improve a low-cost GPS-based collision warning system for vehicle convoys, The Pennsylvania State University, USA, 2010.
15. Won, S.-h. P., Melek, W. W. and Golnaraghi, F., A Kalman/particle filter-based position and orientation estimation method using a position sensor/inertial measurement unit hybrid system. *IEEE Trans. Ind. Electron*., 2010, **57**(5), 1787–1798.
16. Chan, C.-Y., A treatise on crash sensing for automotive air bag systems. IEEE/ASME Transactions on Mechatronics, 2002, **7**(2), 220–234.
17. Zaldivar, J., Calafate, C. T., Cano, J. C. and Manzoni, P., Providing accident detection in vehicular networks through OBD-II devices and Android-based smartphones. In IEEE 36th Conference on Local Computer Networks, Bonn, Germany, 2011.
18. El-Sheimy, N., Hou, H. and Niu, X., Analysis and modeling of inertial sensors using Allan variance. *IEEE Trans. Instrum. Meas.*, 2008, **57**(1), 140–149.
19. Park, S. and Tan, C.-W., GPS-aided gyroscope-free inertial navigation systems. 2002.
20. Park, S. and Tan, C.-W., GPS-aided gyroscope-free inertial navigation systems. California Path Research Report UCB-ITS-PRR-2002-22, Institute of Transportation Studies, University of California, Berkeley, 2002.

Received 17 April 2013; revised accepted 11 April 2014

Simulation study on the photoacoustics of cells with endocytosed gold nanoparticles

Ratan K. Saha*, Madhusudan Roy and Alokmay Datta

Surface Physics and Material Science Division, Saha Institute of Nuclear Physics, 1/AF Bidhannagar, Kolkata 700 064, India

The effect of endocytosis of gold nanoparticles (AuNPs) on photoacoustic (PA) signal is examined using computer simulations. It assumes that the endocytosed AuNPs significantly enhance cellular optical absorption but do not alter thermophysical parameters. The PA signals were computed employing a theoretical model at various cell and intracellular NP concentrations for 532 nm illumination. It was found that the PA amplitude increased linearly in both the cases. The simulation results, when the contributions from both coherent and incoherent components are included, demonstrate good agreement with published experimental results.

Keywords: Computer simulations, endocytosis, gold nanoparticles, photoacoustic signals.

NANOPARTICLES (NPs) are of profound interest in a variety of biological and biomedical studies. Several biomedical imaging modalities use different nanoscale structures such as gold (Au) nanospheres, Au nanorods, silver nanosystems, and carbon (C) nanotubes as contrast enhancers[1,2]. AuNPs are found to be the most suitable for various applications because of their (i) simple and fast preparation procedure, (ii) tunable light scattering and absorbtion properties, (iii) ability to bind with target-specific ligands (through surface roughness manipulation) and (iv) lack of toxicity[1].

Photoacoustic (PA) imaging technique has also extensively used different metallic and non-metallic NPs as contrast agents to improve its sensitivity[3–6]. In PA imaging, a short nanosecond pulsed laser is used to irradiate a tissue sample and this induces a pressure transient due to thermoelastic expansion[7–9]. Such a wide band pressure transient is detected employing an ultrasonic transducer. A raster scan of a 2D region is generally performed to capture PA signals, which are then utilized to generate the corresponding grey scale image. The PA image retains optical contrast of the imaging region, and central frequency of the ultrasonic detector defines resolution of the image. This technique has been widely used to gather anatomical and functional information of various small animal organs at depths beyond optical penetration depth. The administration of NPs allows the PA technique to form images of deep tissue regions with enhanced contrast and this in turn enables it to provide *in vivo* images. Moreover, the capability of the PA technique can be extended to image specific cells or molecules by appropriate surface functionalization of NPs so that they would bind with those cells or molecules and induce PA effect. Various metallic NPs have been employed for visualizing different functional and cellular/molecular processes[10,11]. Studies have also demonstrated that C nanotubes conjugated with cyclic Arg–Gly–Asp (RGD) peptides can serve as contrast agents for PA imaging of tumours[12].

Effort has been made to calculate theoretically the PA pressure emitted by a NP surrounded by a fluid medium[13]. Chen *et al.*[13] computed PA pressure from bare and silica-coated NPs immersed in various solvents and by comparing calculated and measured values revealed that the surrounding medium greatly influences the

*For correspondence. (e-mail: ratank.saha@saha.ac.in)